Photosensitization Aspects of Pinacyanol H-Aggregates. Charge Injection from Singlet and Triplet Excited States into SnO_2 Nanocrystallites

Said Barazzouk,[†,‡] Hong Lee,[‡,§] Surat Hotchandani,[†] and Prashant V. Kamat*[,‡]

Groupe de Recherche en Énergie et Information Biomoléculaires, Université du Québec à Trois Rivières, Trois Rivières, Québec, Canada G9A 5H7, Department of Chemistry, Won Kwang University, Iksan 570-749, Korea, and Notre Dame Radiation Laboratory, Notre Dame, Indiana 46556-0579

Received: December 7, 1999; In Final Form: February 5, 2000

The singlet and triplet excited-state behavior of a symmetric carbocyanine dye, 1,1′-diethyl-2,2′-carbocyanine (commonly referred as pinacyanol), adsorbed on SiO_2 and SnO_2 nanocrystallites has been investigated using transient absorption spectroscopy. The adsorption of the dye molecules on the negatively charged SiO_2 or SnO_2 colloids results in H-type aggregation. When excited with a 532 nm laser pulse we observe a short-lived ($\tau < 30$ ps) singlet excited state of the H-aggregate on the SiO_2 surface. In contrast to this observation, a long-lived cation radical formation is seen on the SnO_2 surface. The dependence of the cation radical yield on the concentration of SnO_2 colloids and the intensity of laser pulse excitation confirms direct electron transfer between the excited aggregate and SnO_2 colloids. Both singlet and triplet excited states of the pinacyanol aggregate participate in the charge injection process on the SnO_2 surface with heterogeneous electron-transfer rate constants of $>5 \times 10^{10}$ and 7×10^9 s^{-1}, respectively. Such a charge injection process is also confirmed from the photocurrent generation at a dye-modified SnO_2 electrode. The fast reverse electron transfer between the photoinjected electron and the cation radical of the dye aggregate is considered to be a major limiting factor in achieving high photoconversion efficiencies.

Introduction

Dye aggregates are useful in developing light-harvesting arrays for artificial photosynthetic systems.[1,2] Use of such dye aggregates as light-harvesting antennas as well as photosensitizers in photoelectrochemical cells have been demonstrated recently.[3,4] Basic understanding of the dye aggregation on a nanoparticle surface as well as the excited-state interaction with the semiconductor support is important in developing efficient photoelectrochemical solar cells.

Carbocyanine dyes have received wide attention because of their application in photodynamic therapy,[5] as a probe of the micellar environment,[6] as initiators in photopolymerization,[7] and as IR absorbing films for optical-disk recording.[8] Pinacyanol (1,1′-diethyl-2,2′-carbocyanine iodide, PCYN), a member of the polymethine class of dyes (Chart 1) is also widely used as a saturable absorber, mode-locker, and sensitizer in imaging technology. Of particular interest is its ability to form H- and J-type aggregates in heterogeneous media.

A strong dispersion force associated with the high polarizability of the chromophoric chain favors aggregation of cyanine dyes in aqueous solution. The high dielectric constant of water facilitates the aggregation process by reducing the electrostatic repulsion between similarly charged dye molecules. Aggregation of these dyes occurs also in mixed solvents[9−12] and in heterogeneous media, e.g., micelles,[13,14] DNA nanotemplates,[15] vesicles,[16] clay,[17] and silica.[18] Spectral shifts or development of new spectral bands in the absorption spectrum often accompanies strong electronic coupling between the molecules in dye aggregates. Both J- and H-type aggregates have been observed for cyanine dyes. For example, 1,1′-diethyl-2,2′-cyanine, or pseudoisocyanine (PIC), exhibits a J-type aggregation with a narrow absorption band at ∼570 nm (red-shifted compared to the monomer band at 523 nm).[19−23] Other carbocyanine dyes, however, exhibit H-type aggregation with a blue-shifted absorption band.[24,25]

CHART 1

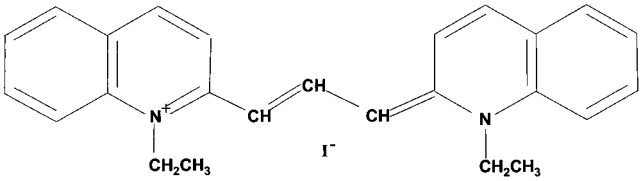

Efforts have been made in recent years to investigate the excited-state dynamics of cyanine dye aggregates in homogeneous media as well as on the surface of silica and AgBr. (See for example, refs 26−38). Cyanine dyes have also been found useful in the investigation of photoisomerization processes,[39−42] yet the information available on the excited-state behavior of these dyes on semiconductor surfaces is rather limited. In the present study we have investigated photophysical, photochemical, and photoelectrochemical properties of PCYN H-aggregates adsorbed on SnO_2 and SiO_2 surfaces using transient absorption spectroscopy. Picosecond dynamics that elucidate the role of the singlet and triplet excited dye aggregates in the charge injection process are presented.

Experimental Section

Materials. PCYN was obtained from Aldrich Chemicals. SnO_2 colloidal suspension (15%, particle diameter 10−15 nm)

* Address correspondence to this author E-mail: pkamat@nd.edu; http://www.nd.edu/∼pkamat.
† Universite du Québec.
‡ Notre Dame Radiation Laboratory.
§ Won Kwang University.

10.1021/jp994311b CCC: $19.00
Published on Web 03/17/2000

was obtained from Alfa Chemicals and used without further purification. SiO_2 colloidal suspension (15%, particle diameter 5 nm) was obtained from NALCO Chemical Co. All the colloidal concentrations indicated in this study are expressed as molecular concentrations. All other chemicals and solvents were analytical reagents of the highest available purity. Optically transparent electrodes (OTE) were cut from an indium tin oxide coated glass plate (1.3 mm thick, 20 Ω/square) obtained from Donnelly Corp., Holland, MI.

OTE/SnO_2 electrode was prepared by casting a thin film of SnO_2 nanoparticles on OTE plates by applying 2% colloidal SnO_2 (Alfa) solution and drying in air.[43] After the electrodes were annealed at 673 K for 1 h, they were modified with PCYN dye. A OTE/SnO_2 electrode was immersed in an aqueous solution of PCYN (0.01−0.1 mM) for 2 h. The adsorption of the dye could visibly be seen as the color of the film changed from colorless to purple. These electrodes are referred to as OTE/SnO_2/PCYN.

Absorption spectra were recorded with a Shimadzu model UV-3101 PC UV−VIS−near-IR scanning spectrophotometer. All the measurements were made in an aqueous medium (pH ≈ 9) at room temperature.

Laser Flash Photolysis Experiments. Nanosecond laser flash photolysis experiments were performed using a 532 nm (second harmonic) laser pulse (~6 ns laser width) from a Quanta Ray model CDR-1 Nd:YAG laser system for excitation.[44] The laser output was suitably attenuated to about 2 mJ/pulse and defocused to minimize the multiphoton process. The experiments were performed in a rectangular quartz cell of 6 mm path length with a right angle configuration between the direction of laser excitation and analyzing light. The photomultiplier output was digitized with a Tektronix 7912 AD programmable digitizer. A typical experiment consisted of a series of five replicate shots per single measurement. The average signal was processed with an LSI-11 microprocessor interfaced to a VAX computer.

Picosecond laser flash photolysis experiments were performed with 532 nm laser pulses from a mode-locked, Q-switched Continuum YG-501 DP Nd:YAG laser system (output 2 mJ/pulse, pulse width ~18 ps). Passing the fundamental output through a D_2O/H_2O solution generated the white continuum picosecond probe pulse. The output was fed to a spectrograph (HR-320, ISDA Instruments, Inc.) with fiber optic cables and was analyzed with a dual diode array detector (Princeton Instruments, Inc.) interfaced with a PC. The details of the experimental setup and its operation are described elsewhere.[45,46] Time zero in these experiments corresponds to the end of the excitation pulse. All the lifetimes and rate constants reported in this study have an experimental error of ±5%.

Photoelectrochemical Experiments. The measurements were carried out in a thin-layer cell consisting of a 5 mm path length quartz cuvette with two side arms attached for inserting reference (Ag/AgCl or SCE) and counter (Pt gauze) electrodes. The cell design is described elsewhere.[43] A Princeton Applied Research (PAR) model 173 potentiostat and model 175 universal programmer were used in the photoelectrochemical measurements. Photocurrent measurements were carried out with a Kiethley model 617 programmable electrometer. The collimated light beam was from a 250 W xenon lamp. A Bausch and Lomb high-intensity grating monochromator was introduced into the path of the excitation wavelength. The illuminated area of the electrode was approximately 1 cm^2, which is approximately half the area of the dye-modified SnO_2 film.

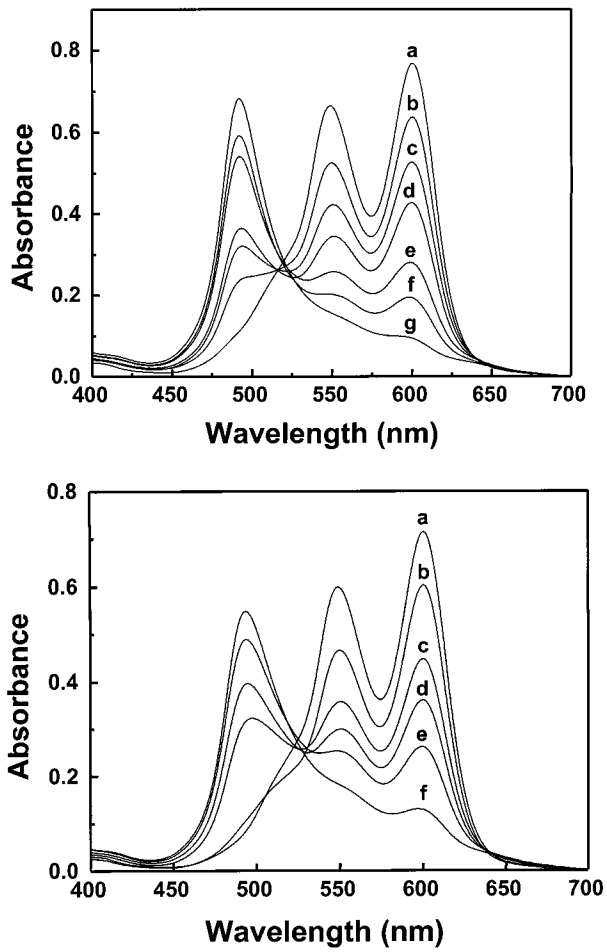

Figure 1. (A, top) Absorption spectra of aqueous PCYN (13.9 μM) at various amounts of SnO_2 colloids: (a) 0, (b) 43, (c) 86, (d) 107.5, (e) 172, (f) 258, and (g) 344 μM. (B, bottom) Absorption spectra of, aqueous PCYN (13.9 μM) at various amounts of SiO_2 colloids: (a) 0, (b) 23.8, (c) 166.8, (d) 190.7, (e) 214.5, and (f) 238 μM.

Results

Aggregation of PCYN on SiO_2 and SnO_2 Colloids. PCYN is a cationic dye that exhibits two strong absorption bands in the visible with maxima at 600 and 550 nm in aqueous solution. Parts A and B of Figure 1 show the absorption changes observed upon adsorption of the dye molecules on the negatively charged SnO_2 and SiO_2 colloids, respectively. We observe a blue shift in the absorption maximum (abs max ≈ 495 nm) in both these experiments. The monomer absorption bands at 600 and 550 nm decrease with simultaneous appearance of a new absorption band at 495 nm as the dye molecules are adsorbed on SiO_2 and SnO_2 nanoparticles. The observation of an isosbestic point at ~525 nm in these spectra further supports the argument that the monomer and aggregate forms of the dye are in equilibrium (eq 1).

$$\mathrm{PCYN} + \mathrm{SnO_2} \leftrightarrow \mathrm{PCYN\cdots SnO_2} \overset{\mathrm{PCYN}}{\rightleftharpoons} (\mathrm{PCYN})_2\cdots\mathrm{SnO_2} \quad (1)$$

The initial step of dye adsorption on the colloidal SiO_2 or SnO_2 particle surface involves strong electrostatic interactions. Intermolecular interaction between the neighboring dye molecules on the oxide surface results in aggregation effects. The shift of the absorption band to the higher energy region confirms the aggregation to be the H-type. (Note that for H-type

aggregates, the transition to the upper excitonic state S^{+}_{1} is only allowed.) Similar H-type aggregation has been observed for several cationic dyes (rhodamine, cresyl violet, and thionine) adsorbed on various oxide surfaces.[27,28,47,48] Such an H-type aggregation represents a sandwich-type stacking of dye molecules on the surfaces of SiO_2 and SnO_2 nanoparticles.

At higher support concentrations, some deviation in the isosbestic point is noticeable. This we attribute to the possible dissociation of larger aggregates. Although few previous studies have succeeded in resolving absorption bands due to larger aggregates,[49] we were not able to resolve the overlapping transitions arising from different aggregates (dimer, trimer, etc.). The appearance of an aggregate absorption band even at low dye concentrations suggests that the distribution of dye molecules on the SiO_2 and SnO_2 colloid surface is not random, but they are bound preferentially to adjacent surface sites as pointed out by Bergman and O'Konski.[50] Similar observation was also made by Quitevis and co-workers in their study on the H-aggregates of 1,1′-diethyl-2,2′-dicarbocyanine (DDC) on colloidal silica.[34] They argued that aggregation would not be possible at very low coverage if the molecules were randomly distributed on the colloid surface. The aggregation in the present experiments occurred because of favorable dispersion interactions on SiO_2 and SnO_2 colloids.

Excited Singlet States of Monomer and H-Aggregate Forms of PCYN. Both the monomer and H-aggregate of PCYN do not exhibit any noticeable fluorescence under visible light excitation. This implies that internal conversion, intersystem crossing, and isomerization dominate the quick deactivation of the excited singlet state. Figure 2 shows the difference absorption spectra recorded following 532 nm laser pulse (pulse width 18 ps) excitation of PCYN in aqueous solution. The singlet excited state of the monomer form of the dye exhibits an absorption maximum at 460 nm and ground state depletion at wavelengths greater than 500 nm. The presence of an isosbestic point at 500 nm indicates the conversion of the ground-state dye into an excited singlet following 532 nm laser excitation. The absorption band at 460 nm decays quickly as the singlet excited state gets deactivated. The lifetime of the singlet excited state as measured from the first-order decay of the transient absorption at 460 nm (Figure 2) is 140 ps and matches well with the lifetime (149 ps) obtained from the recovery of the bleaching.

A few recent studies report photophysical aspects of different cyanine dye aggregates.[26,38,51] Many of these studies have employed relatively high dye concentrations or altered the medium (e.g., addition of salts) to induce aggregation. Such an approach does not exclusively rule out the contribution from the excited monomer since the monomer form remains in equilibrium with the aggregate form. However, adsorption of the cyanine dye on SiO_2 or SnO_2 colloids yields aggregates even at very low dye concentrations. In an earlier study, Quitevis and co-workers[34] have employed a similar approach to investigate the excited-state behavior of DDC dye aggregates on SiO_2 colloids. To investigate the singlet excited-state properties of H-aggregates of PCYN, we excited the dye aggregates formed in colloidal SiO_2 suspension. Since SiO_2 is an inert support, it does not directly influence the excited-state properties of adsorbed dye molecules.

The difference absorption spectra of the excited singlet state of H-aggregates of PCYN in SiO_2 suspension are shown in Figure 3. The difference absorption spectra recorded immediately after 532 nm laser pulse excitation show an intense bleaching at wavelengths greater than 450 nm. The transient

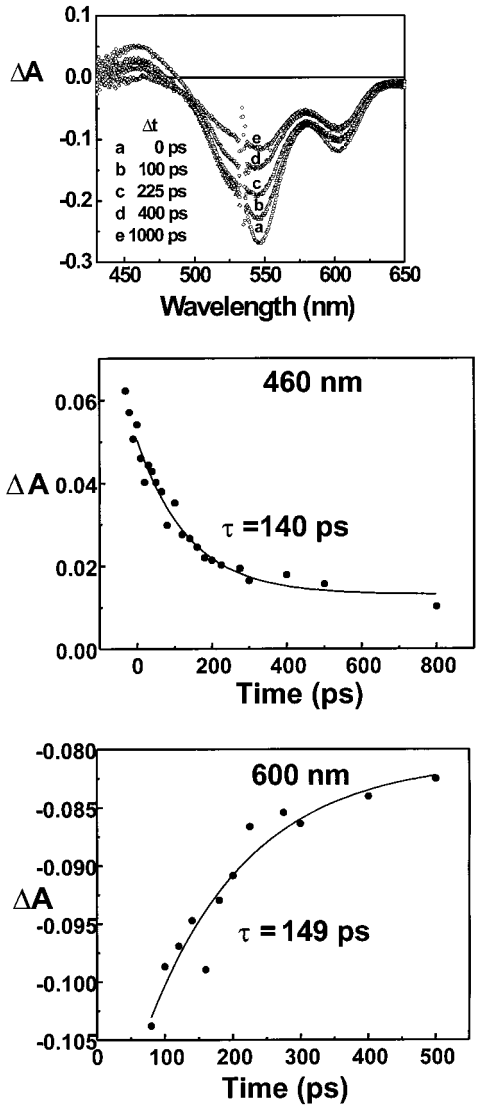

Figure 2. (top) Transient absorption spectra of aqueous PCYN (20.8 μM) recorded (a) 10, (b) 100, (c) 225, (d) 400, and (e) 1000 ps after 532 nm laser pulse excitation. Absorption time profile spectra recorded following 532 laser pulse excitation of aqueous PCYN (20.8 μM) at (middle) 460 nm and (bottom) 600 nm.

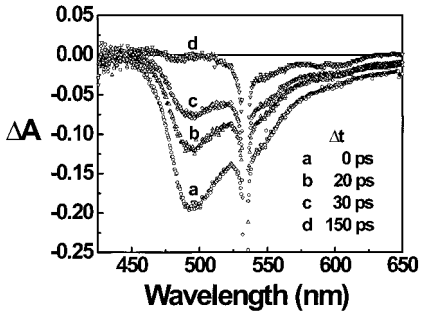

Figure 3. Transient absorption spectra of an aqueous solution containing 20.8 μM PCYN and 238 μM SiO_2 recorded (a) 0, (b) 20, (c) 30, and (d) 150 ps after 532 nm laser pulse excitation.

bleaching with a maximum around 500 nm confirms the depletion of the ground state as it gets converted into the singlet excited state. Absence of a positive absorbance in the difference absorption spectrum (Figure 3) indicated that the extinction coefficient of the excited singlet is smaller than the ground state of $(PCYN)_2$ in the visible region.

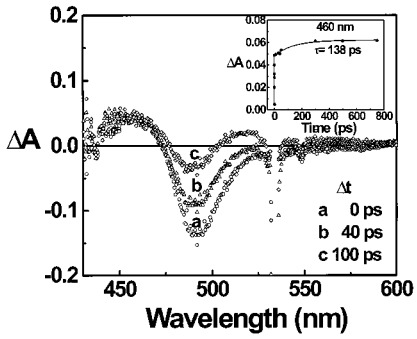

Figure 4. Transient absorption spectra of an aqueous solution containing 20.8 μM PCYN and 344 μM SnO_2 recorded at (a) 0, (b) 40, and (c) 100 ps after 532 nm laser pulse excitation. Absorption time profile recorded at 460 nm following 532 laser pulse excitation of an aqueous solution containing 20.8 μM PCYN and 344 μM SnO_2 is shown in the inset.

As discussed earlier,[52−54] the internal conversion from the upper lying state S^+_1 to the lower lying state S^-_1 is an ultrafast process which is completed within the laser pulse duration of 20 ps (eq 2). The decay of the excited singlet state observed in the present experiment essentially corresponds to the intersystem crossing process that leads to the formation of the triplet excited state (eq 3). It may be noted that direct conversion from S^-_1 to S_0 is considered to be a forbidden transition in the case of H-aggregates.

$$(PCYN)_2 + h\nu \rightarrow {}^1(PCYN)_2^*\,(S^+_1) \rightarrow {}^1(PCYN)_2^*\,(S^-_1) \quad (2)$$

$${}^1(PCYN)_2^*\,(S^-_1) \rightarrow {}^3(PCYN)_2^* \quad (3)$$

The recovery of bleaching of the 490 nm band is very fast and is completed within the duration of ~100 ps. We expect the lifetime of the H-aggregate to be less than 30 ps in colloidal SiO_2 suspension. Quitevis and co-workers[34] have found a distribution of cyanine dye aggregates with different lifetimes ranging from 20 to 200 ps in colloidal SiO_2 suspension. The residual bleaching observed at longer time (spectrum d in Figure 3) essentially shows the formation of the triplet excited state of the aggregate.

Charge Injection into SnO_2 Nanoparticles. Semiconducting oxides such as TiO_2 and SnO_2 directly interact with the excited dye molecules to induce heterogeneous electron transfer at the semiconductor/dye interface. This interesting property of sensitizing dyes is useful in the design of photochemical solar cells.[55] In a recent study we have shown that the excited dye aggregates can also independently compete with the excited monomers in the charge injection process.[4,56] Moreover, the charge transfer between the excited dye aggregate and the silver halide is considered to be an important photochemical step in photographic applications. Such an interesting behavior of dye aggregates has prompted the investigation of excited-state behavior of cyanine and other classes of dyes on semiconductor surfaces.[57,58]

Time-resolved transient absorption spectra recorded after 532 nm laser pulse excitation of $(PCYN)_2$ adsorbed on SnO_2 colloids are shown in Figure 4. The difference absorption spectrum recorded immediately after laser pulse excitation exhibits an absorption maximum at 460 nm. This transient absorption survives longer than the singlet excited lifetimes and does not decay even at times greater than 500 ps. We attribute this absorption band to the formation of the cation radical of the $(PCYN)_2$, an electron-transfer product of the charge injection process (reaction 4).

$${}^1(PCYN)_2^* + SnO_2 \rightarrow (PCYN)_2^{\bullet+} + SnO_2\,(e) \quad (4)$$

The absorption−time profile recorded at 460 nm is shown in the inset of Figure 4. More than half of the absorption signal was prompt, indicating the formation of this transient within the laser pulse duration of 20 ps. A slow growth component also follows this signal with a lifetime of about 140 ps. The fast component arises as a result of charge injection from the excited singlet of $(PCYN)_2$. (It may be recalled that we observed a fast decay of the excited singlet in the SiO_2 system, which disappeared within a time frame of 100 ps.) Thus, we expect the electron-transfer rate constant for the charge injection from the excited singlet to be greater than 5×10^{10} s^{-1}, the resolution of which is limited by the pulse width of the excitation pulse. Earlier studies carried out with various dyes on semiconductor surfaces and their aggregates have shown that the charge injection process occurs over a femtosecond to picosecond time scale.[29,35,37,59−63]

Although surface heterogeneity can contribute to slower charge injection rates,[64] it is not the principal reason for the observed slow rise in $(PCYN)_2^{\bullet+}$ formation. The singlet excited-state lifetime is too short (≤30 ps) to match the rise time (140 ps) of the slow-growth component in Figure 4. Hence, the slower growth of cation radical absorption (lifetime of 140 ps) represents the contribution from the reaction of the long-lived triplet excited state with SnO_2 colloids. The rate constant for the charge injection from the triplet excited state is $\sim 7 \times 10^9$ s^{-1}, a value significantly smaller than the one observed for the singlet excited state ($k_{et} > 5 \times 10^{10}$ s^{-1}). Triplet excited states are known to get populated in H-type aggregates because of the forbidden S_1-S_0 transition. Compared to the singlet excited state, the triplets are long-lived and hence are capable of injecting electrons even from a weakly coupled state. There are a few citations of charge injection from the excited triplet state into the large band gap semiconductor that exhibit a relatively slower rate of electron injection than the singlet excited state.[27,59,65−68]

Role of Oxide Support in Inducing Excited-State Electron Transfer. Oxide supports play an important role in controlling the excited-state behavior of adsorbed molecules. The charge injection process as discussed in the previous section is usually encountered with oxide supports that exhibit semiconducting properties. Figure 5 shows transient absorption spectra recorded immediately after 532 nm laser pulse (pulse width 6 ns) excitation of $(PCYN)_2/SnO_2$ colloids. The difference absorption spectrum recorded immediately after the laser pulse excitation shows the formation of $(PCYN)_2^{\bullet+}$ with an absorption maximum around 450 nm and a bleaching at 490 nm. Although a major fraction of the transient absorption decays during the first few nanoseconds, we were able to characterize the electron-transfer products in our nanosecond laser flash photolysis set up. The inset in Figure 5 shows the dependence of $(PCYN)_2^{\bullet+}$ on the laser excitation intensity. The linear dependence of the electron-transfer yield confirms that reaction 4 is a monophonic process.

Other surface photochemical processes such as photoionization could also produce $(PCYN)_2^{\bullet+}$ on oxide surfaces. The insulating oxide materials such as SiO_2 have a large band gap and cannot be sensitized with organic dyes. However, we can observe a biphotonic ionization of PCYN if we increase our laser excitation intensity by 10-fold (~20 mJ/pulse). The photoproduct, $(PCYN)_2^{\bullet+}$, observed in this case also had spectral

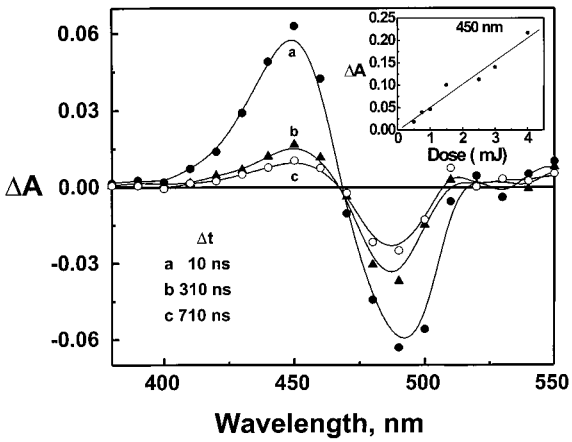

Figure 5. Time-resolved transient absorption spectra recorded following 532 laser pulse excitation of an aqueous solution containing 20.8 μM PCYN and 344 μM SnO_2. The spectra were recorded at Δt = 10, 310, and 710 ns after laser pulse excitation. The inset shows the dependence of the cation radical yield, at 450 nm, on the relative laser dose.

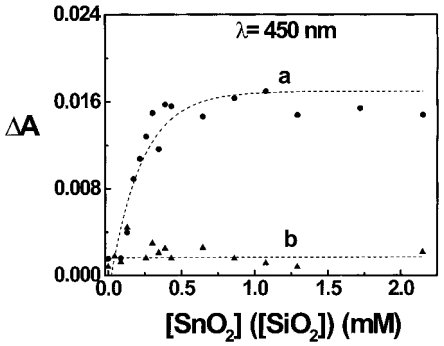

Figure 6. Dependence of transient absorbance at 450 nm on the concentration of (a) SnO_2 and (b) SiO_2 colloids. The concentration of PCYN (20.8 μM) and excitation laser intensity (~2 mJ) were kept constant.

features similar to those illustrated in Figure 5. In all our experiments we employed low excitation intensity (~2 mJ) to minimize any multiphotonic processes.

Figure 6 shows the dependence of $(PCYN)_2^{\bullet+}$ yield on the concentration of SnO_2 and SiO_2 colloids. The transient absorbance (450 nm) recorded immediately after the laser pulse excitation was monitored at different colloid concentration while the dye concentration was kept constant. In the absence of SnO_2 or SiO_2 colloids there is no detectable transient absorption at 450 nm, thus ruling out any possible contribution from the monomeric form of the dye. With increasing SnO_2 colloid concentration the transient absorbance at 450 nm increases as more dye molecules aggregate and participate in the charge injection process. At concentrations greater than 0.5 mM SnO_2, the yield of $(PCYN)_2^{\bullet+}$ saturates as all the dye molecules get adsorbed on the SnO_2 particles and participate in the charge injection process. The experiments carried out with SiO_2 colloids using the same conditions did not exhibit any detectable yield of $(PCYN)_2^{\bullet+}$. These observations confirm direct participation of SnO_2 colloids in deactivating excited dye aggregates via the electron-transfer pathway.

Reverse Electron Transfer between $(PCYN)_2^{\bullet+}$ and Injected Electrons. We also probed the decay of the cation radical of the dye aggregate, $(PCYN)_2^{\bullet+}$, in a nanosecond laser flash photolysis apparatus. Figure 7 shows the absorption−time profiles of $(PCYN)_2^{\bullet+}$ monitored at 450 and 490 nm. The rapid decay of $(PCYN)_2^{\bullet+}$ arises from the reverse electron transfer

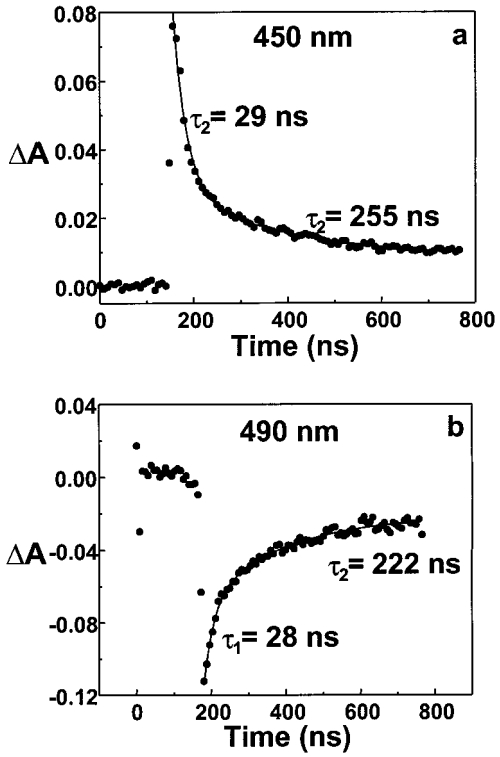

Figure 7. Absorption time profiles recorded following 532 laser pulse excitation of an aqueous solution containing 20.8 μM PCYN and 344 μM SnO_2 at (a) 450 and (b) 490 nm.

with injected electrons (reaction 5). The transient absorbance-

$$(PCYN)_2^{\bullet+} + SnO_2\,(e) \rightarrow (PCYN)_2 + SnO_2 \qquad (5)$$

time profile of $(PCYN)_2^{\bullet+}$ exhibits multiexponential decay behavior and can be fitted to a biexponential kinetic fit. The two lifetimes, 29 and 255 ns, obtained from this analysis show the upper and lower limits for the reverse electron transfer. The heterogeneity of the surface and the nature of trapped sites render the heterogeneous electron-transfer kinetics a more complex behavior.

Photosensitized Current Generation in PCYN-Modified SnO_2 Electrodes. The photosensitization aspect of PCYN aggregates was further evaluated by adsorbing the dye onto nanostructured SnO_2 films. When OTE/SnO_2 electrodes (see the Experimental Section for the method of preparation) was immersed in an aqueous solution containing PCYN, the color of the SnO_2 film changed to purple as the dye from solution was adsorbed. Figure 8A shows the absorption spectra of OTE/SnO_2 electrodes after immersion in an aqueous solution containing different concentrations of PCYN. In all four cases the absorption peak of $(PCYN)_2$ at ~495 nm was prominently seen along with the monomer peaks at 550 and 600 nm. The ratio of aggregate to monomer absorption maxima ($A_{495\ nm}/A_{600\ nm}$) increased from 0.8 to 1.5 as we adsorb increasing amounts of dye onto the SnO_2 film. As discussed in the previous sections, the intermolecular interactions between the adsorbed dye molecules lead to the aggregation effects.

When we employ the OTE/SnO_2/$(PCYN)_2$ electrode as a photoanode in a photoelectrochemical cell, prompt photocurrent generation can be seen. The photocurrent action spectrum shown in Figure 8B confirms the participation of both monomer and aggregate forms of PCYN. It is interesting to note that the photocurrent generation efficiency (IPCE) at 490 nm is significant even at low dye coverage. This further confirms that the

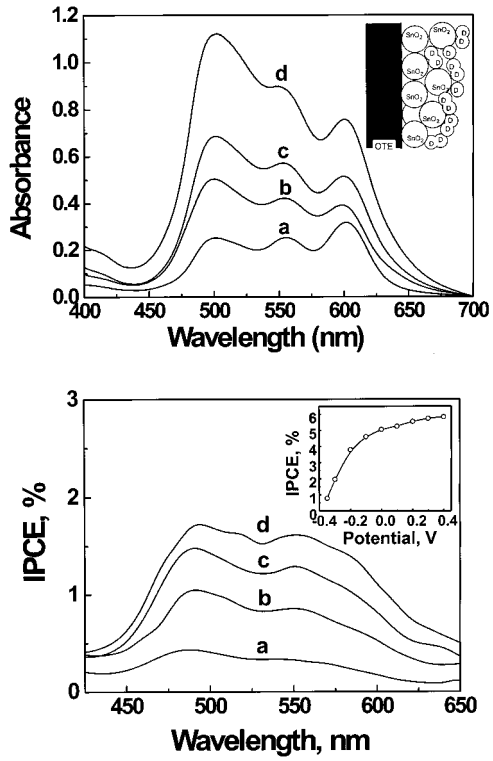

Figure 8. (A, top) Absorption spectra of PCYN adsorbed on nanostructured SnO_2 films. The adsorption of the dye was carried out by immersing OTE/SnO_2 electrodes in a solution containing (a) 21, (b) 42, (c) 63, and (d) 84 μM dye in water for 2 h. (B, bottom) Photocurrent action spectra of PCYN modified electrodes using 0.5 M LiI in acetonitrile. The inset shows the dependence of IPCE (at 495 nm) on the applied potential (CE, Pt; RE, Ag/AgCl). (The incident photon to photocurrent generation efficiency was determined from the expression IPCE% = $(1240/\lambda)(i_{sc}/I_{inc}) \times 100$.)

dye aggregates directly compete with the monomers to inject electrons into SnO_2 nanocrystallites. Although the IPCE maximum is low compared to those of other organic sensitizers (less than 2%), these experiments show the possibility of employing cyanine dye aggregates as photosensitizers. The IPCE can be improved further by application of an applied bias (see the inset in Figure 8B). At potentials greater than the flat band potential of SnO_2 ($\sim$0 V vs NHE), we observe an enhanced IPCE value at 495 nm excitation.

Discussion

The binding of cyanine dye molecules to the SiO_2 and SnO_2 surface induces intermolecular interactions leading to an aggregation effect. The blue shift in the absorption band confirms the dye aggregation to be the H-type. The singlet excited state of the H-aggregate is short-lived as it quickly undergoes intersystem crossing to generate triplet excited state. Both singlet and triplet excited H-aggregates of PCYN are capable of injecting electrons into large band gap semiconductor material such as SnO_2.

One of the major factors influencing the reactivity of the excited states of the sensitizer is the type of interaction between the dye and the semiconductor surface. In the case where strong electronic coupling between the excited dye and the semiconductor surface dominates, one observes electron transfer in less than 100 fs.[60−62,69] Such a strong coupling is considered to be an essential factor in maximizing the photosensitization efficiency of photochemical solar cells. In the present experiments the interactions between the dye aggregates and SnO_2 colloid

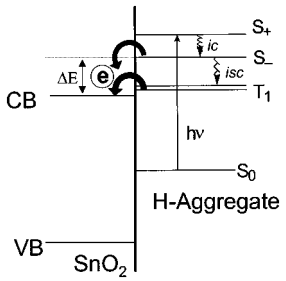

Figure 9. Participation of singlet and triplet excited states of the dye aggregate in the charge injection process.

are significantly weaker than the ones achieved via charge-transfer interactions using carboxylate or phosphonate functional groups of sensitizing dye molecules. Thus, the charge injection process from the singlet excited dye aggregate directly competes with intersystem crossing. Excited triplets thus accumulated during the deactivation of the singlet excited state also participate in the charge injection process, but at a slower rate. The participation of singlet and triplet excited states in the charge injection process are illustrated in Figure 9.

The energy difference between the excited states and the conduction band of SnO_2 plays a major role in controlling the kinetics of the charge-transfer process. The oxidation potential of PCYN is +0.47 V vs SCE. By considering the singlet-state energy of PCYN as $\sim$2.0 eV, we estimate the oxidation potential of the excited state to be around −1.53 V. This energy level is more negative than the conduction band energy of SnO_2 (−0.35 V vs SCE at pH 9).[70] The difference in energy between the two provides the necessary driving force for the charge injection process. In our previous study with the ruthenium(II) polypyridyl complex, adsorbed on different semiconductors, we showed that the interfacial electron-transfer rate constant is strongly dependent on the energy difference between the conduction band of the semiconductor and the oxidation potential of the excited dye.[71] As can be seen from Figure 9, the driving force for the electron transfer from the excited singlet dye into the SnO_2 semiconductor is rather high ($\Delta E \approx 1.177$ V vs SCE). This energy difference is expected to decrease for the charge injection from the triplet excited state.

As a result of this we see both singlet and triplet excited states injecting electrons with rate constants of $>(5 \pm 0.1) \times 10^{10}$ and $(7 \pm 0.1) \times 10^9$ s^{-1}, respectively. It is interesting to note that the charge injection rate constant for the triplet excited state is nearly an order of magnitude smaller than that of the singlet excited state. The weaker semiconductor−dye interactions and decreased energy difference between the oxidation potential of the triplet excited dye and the conduction band of SnO_2 are the likely factors influencing slower charge-transfer kinetics. Similar slower charge injection from the triplet excited state has been reported for other organic dyes.[66,67,72]

The SnO_2 thin-film electrodes modified with PCYN aggregates exhibit low photocurrent conversion efficiencies (<6%). An important criterion for achieving better power conversion efficiencies in photochemical solar cells is to stabilize the injected charge in the semiconductor nanocrystallites. This enables the injected charge to migrate through the particulate film to the collecting surface of the electrode. The reverse electron transfer between the injected electron and the cation radical of the sensitizer can limit the efficiency if it is not suppressed effectively. Often, the use of a redox couple (e.g., I_3^-/I^-) minimizes the loss due to reverse electron transfer by quickly regenerating the sensitizer. This technique is considered to be effective for ruthenium(II) polypyridyl/TiO_2 based sys-

tems.[73] However, for organic dye based systems the rate constant for the reverse electron transfer is 2−3 orders of magnitude faster than the one observed for the sensitization of SnO_2 and TiO_2 colloids with a ruthenium(II) bipyridyl complex.[56] It is evident that the fast reverse electron transfer in the $(PCYN)_2/SnO_2$ system ($k_{ret} = (0.4-3) \times 10^7\ s^{-1}$) is a limiting factor in achieving charge stabilization since it directly competes with the sensitizer regeneration via a redox couple in the electrolyte. The photoelectrochemical measurements carried out under applied bias (inset in Figure 8B) further support this argument. At potentials more positive than the flat band potential of SnO_2, we observe an increase in IPCE. By introducing additional driving force within the SnO_2 film, we increase the probability of the injected electrons to reach the collecting surface of OTE.

Conclusions

H-type aggregation effects are seen on SiO_2 and SnO_2 nanoparticles when PCYN molecules are adsorbed with favorable disperse interactions. The singlet excited monomer and H-aggregate of PCYN are short-lived with lifetimes of 140 and <30 ps, respectively. SnO_2 nanoparticles directly interact with the excited aggregate, while SiO_2 particles remain inert. The charge injection from the excited dye aggregate into SnO_2 nanocrystallites is marked by the formation of the cation radical $(PCYN)_2^{\bullet+}$. The rate constant of reverse electron transfer between the injected electron and the cation radical of the dye aggregate remains to be significantly high and thus makes this process a major limiting factor for achieving high photoconversion efficiencies.

Acknowledgment. We acknowledge the support of the Office of Basic Energy Science of the U.S. Department of Energy (P.V.K.), Won Kwang University, Iksan, Korea (H.L.), and Natural Sciences and Engineering Research Council of Canada (S.B. and S.H.) to carry out this work. This is Contribution No. 4155 from the Notre Dame Radiation Laboratory.

References and Notes

(1) Muniro, M.; Nozawa, T.; Tamai, N.; Shimada, K.; Yamazaki, I.; Lin, S.; Knox, R. S.; Wittershaus, B. P.; Brune, D. C.; Blankenship, R. E. *J. Phys. Chem.* **1989**, *93*, 7503−7509.
(2) Wang, Y. *Chem. Phys. Lett.* **1986**, *126*, 209.
(3) Das, S.; Kamat, P. V. *J. Phys. Chem. B* **1999**, *103*, 209−215.
(4) Khazraji, A. C.; Hotchandani, S.; Das, S.; Kamat, P. V. *J. Phys. Chem. B* **1999**, *103*, 4693−4700.
(5) Krieg, M.; Redmond, R. W. *Photochem. Photobiol.* **1993**, *57*, 472−479.
(6) Grieser, F.; Lay, M.; Thistlethwaite, P. J. *J. Phys. Chem.* **1985**, *89*, 2065−2070.
(7) Chatterjee, S.; Sarkar, S.; Bhattacharyya, S. N. *J. Photochem. Photobiol., A* **1994**, *81*, 199−203.
(8) Matsui, F. *Optical recording Systems*; Plenum: New York, 1990.
(9) Selwyn, J. E.; Steinfeld, J. I. *J. Phys. Chem.* **1972**, *76*, 762−774.
(10) Arbeloa, F. L.; Gonzalez, I. L.; Ojeda, P. R.; Arbeloa, I. L. *J. Chem. Soc., Faraday Trans. 2* **1982**, *78*, 989−994.
(11) Arbeloa, F. L.; Ojeda, P. R.; Arbeloa, I. L. *J. Chem. Soc., Faraday Trans. 2* **1988**, *84*, 1903−1912.
(12) Arbeloa, F. L.; Arbeloa, T. L.; Lage, E. G.; Arbeloa, I. L.; De Schryver, F. C. *J. Photochem. Photobiol., A* **1991**, *56*, 313.
(13) Kelkar, V. K.; Valalulikar, B. S.; Kunjappu, J. T.; Manohar, C. *Photochem. Photobiol.* **1990**, *52*, 717−721.
(14) Mialocq, J. C.; Hebert, P.; Armand, X.; Bonneau, R.; Morand, J. P. *J. Photochem. Photobiol., A* **1991**, *56*, 323−38.
(15) Seifert, J. L.; Conner, R. E.; Kushon, S. A.; Wang, M.; Armitage, B. A. *J. Am. Chem. Soc.* **1999**, *121*, 2987−2995.
(16) Deumie, M. D.; Lorente, P.; Morizon, D. *Photochem. Photobiol., A* **1995**, *89*, 239−245.
(17) Arbeloa, F. L.; Estevez, M. J. T.; Arbeloa, T. L.; Arbeloa, I. L. *Langmuir* **1995**, *11*, 3211−3217.
(18) Avnir, D.; Levy, D.; Reisfeld, R. *J. Phys. Chem.* **1984**, *88*, 5956−9.
(19) Jelly, E. E. *Nature (London)* **1936**, *138*, 1009.
(20) Scheibe, G. *Angew. Chem.* **1936**, *49*, 563.
(21) Mattoon, R. W. *J. Chem. Phys.* **1944**, *12*, 268.
(22) Zimmermann, H.; Scheibe, G. *Z. Electrochem.* **1956**, *60*, 566.
(23) Cooper, W. *Chem. Phys. Lett.* **1970**, *7*, 73.
(24) Emerson, E. S.; Conlin, M. A.; Rosenoff, A. E.; Norland, K. S.; Rodriguez, H.; Chin, C.; Bird, G. R. *J. Phys. Chem.* **1967**, *71*, 2396.
(25) West, W.; Pearce, S. *J. Phys. Chem.* **1965**, *69*, 1894−1903.
(26) Khairutdinov, R. F.; Serpone, N. *J. Phys. Chem. B* **1997**, *101*, 2602−2610.
(27) Liu, D.; Kamat, P. V. *J. Chem. Phys.* **1996**, *105*, 965−970.
(28) Liu, D.; Hug, G. L.; Kamat, P. V. *J. Phys. Chem.* **1995**, *99*, 16768−16775.
(29) Martini, I.; Hartland, G.; Kamat, P. V. *J. Phys. Chem. B* **1997**, *101*, 4826−4830.
(30) Watanabe, M.; Herren, M.; Morita, M. *J. Lumin.* **1994**, *58*, 198−201.
(31) Horng, M.-L.; Quitevis, E. L. *J. Phys. Chem.* **1989**, *93*, 6198−6201.
(32) Quitevis, E. L.; Horng, M.-L.; Chen, S.-Y. *J. Phys. Chem.* **1988**, *92*, 256.
(33) Kemnitz, K.; Yoshihara, K.; Ohzeki, K. *J. Phys. Chem.* **1990**, *94*, 3099−3104.
(34) Chen, S.-Y.; Horng, M.-L.; Quitevis, E. L. *J. Phys. Chem.* **1989**, *93*, 3683−3688.
(35) Butoi, C. I.; Langdon, B. T.; Kelley, D. F. *J. Phys. Chem. B* **1998**, *102*, 9635−9639.
(36) Trosken, B.; Wiilig, F.; Schwarzburg, K.; Ehret, A.; Spitler, M. *J. Phys. Chem.* **1995**, *99*, 5152−5160.
(37) Tani, T.; Suzumoto, T.; Kemnitz, K.; Yoshihara, K. *J. Phys. Chem.* **1992**, *96*, 2778−2783.
(38) Serpone, N.; Sahyun, M. R. V. *J. Phys. Chem.* **1994**, *98*, 734−737.
(39) Martin, M. M.; Plaza, P.; Meyer, Y. H. *Chem. Phys.* **1995**, *192*, 367−77.
(40) Chibisov, A. K.; Zakharova, G. V.; Goerner, H.; Sogulyaev, Y. A.; Mushkalo, I. L.; Tolmachev, A. I. *J. Phys. Chem.* **1995**, *99*, 886−93.
(41) Di Paolo, R. E.; Scaffardi, L. B.; Duchowicz, R.; Bilmes, G. M. *J. Phys. Chem.* **1995**, *99*, 13796−13799.
(42) Onganer, Y.; Yin, M.; Bessire, D. R.; Quitevis, E. L. *J. Phys. Chem.* **1993**, *97*, 2344−2354.
(43) Bedja, I.; Hotchandani, S.; Kamat, P. V. *J. Phys. Chem.* **1994**, *98*, 4133−4140.
(44) Nagarajan, V.; Fessenden, R. W. *J. Phys. Chem.* **1985**, *89*, 2330−2335.
(45) Ebbesen, T. W. *Rev. Sci. Instrum.* **1988**, *59*, 1307−1309.
(46) Kamat, P. V.; Ebbesen, T. W.; Dimitrijevic, N. M.; Nozik, A. J. *Chem. Phys. Lett.* **1989**, *157*, 384−9.
(47) Liu, D.; Kamat, P. V. *Langmuir* **1996**, *12*, 2190−2195.
(48) Nasr, C.; Liu, D.; Hotchandani, S.; Kamat, P. V. *J. Phys. Chem.* **1996**, *100*, 11054−11061.
(49) Hyungsik, M.; Jeunghee, P.; Jongwan, Y.; Dongho, K. *Bull. Korean Chem. Soc.* **1998**, *Vol. 19*, 650−654.
(50) Bergmann, K.; O'Konski, C. T. *J. Phys. Chem.* **1963**, *67*, 2169−2177.
(51) Gomes, A. S. L.; Taylor, J. R. *J. Photochem.* **1986**, *32*, 325.
(52) McRae, E. G.; Kasha, M. The Molecular Exciton Model. In *Physical Processes in Radiation Biology*; Augenstein, L., Mason, R., Rosenberg, B., Eds.; Academic Press: New York, 1964; pp 23−42.
(53) Kasha, M.; Rawls, H. R.; El-Bayoumi, M. A. *Pure Appl. Chem.* **1965**, *11*, 371−392.
(54) Scherer, P. O. J.; Fisher, S. F. *Chem. Phys.* **1984**, *86*, 269.
(55) Grätzel, M. Nanocrystalline electronic junctions. In *Semiconductor Nanoclusters—Physical, Chemical and Catalytic Aspects.*; Kamat, P. V., Meisel, D., Eds.; Elsevier Science: Amsterdam, 1997; pp 353−375.
(56) Liu, D.; Fessenden, R. W.; Hug, G. L.; Kamat, P. V. *J. Phys. Chem. B* **1997**, *101*, 2583−2590.
(57) Kietzmann, R.; Ehret, A.; Spitler, M.; Willig, F. *J. Am. Chem. Soc.* **1993**, *115*, 1930−6.
(58) Trosken, B.; Willig, F.; Schwarzburg, K. *J. Phys. Chem.* **1995**, *99*, 5152−5160.
(59) Eichberger, R.; Willig, F. *Chem. Phys. Lett.* **1990**, *141*, 159−73.
(60) Tachibana, Y.; Moser, J. E.; Grätzel, M.; Klug, D. R.; Durrant, J. R. *J. Phys. Chem.* **1996**, *100*, 20056−20062.
(61) Hannappel, T.; Burfeindet, B.; Storck, W.; Willig, F. *J. Phys. Chem. B* **1997**, *101*, 6799−6802.
(62) Randy, J.; Ellingson, R. J.; Asbury, J. B.; Ferrere, S.; Ghosh, H. N.; Sprague, J. R.; Lian, T.; Nozik, A. J. *J. Phys. Chem. B* **1998**, *102*, 6455−6458.

(63) Asbury, J. B.; Wang, Y. Q.; Lian, T. *J. Phys. Chem. B* **1999**, *103*, 6643−6647.
(64) Fessenden, R. W.; Kamat, P. V. *J. Phys. Chem.* **1995**, *99*, 12902−12906.
(65) Willig, F.; Eichberger, R.; Sundaresan, N. S.; Parkinson, B. A. *J. Am. Chem. Soc.* **1990**, *112*, 2702−7.
(66) Ryan, M. A.; Fitzgerald, E. C.; Spitler, M. T. *J. Phys. Chem.* **1989**, *93*, 6150−6.
(67) Patrick, B.; Kamat, P. V. *J. Phys. Chem.* **1992**, *96*, 1423−8.
(68) Zang, L.; Rodgers, M. A. J. *J. Phys. Chem. B* **2000**, *104*, 468−474.
(69) Martini, I.; Hodak, J.; Hartland, G.; Kamat, P. V. *J. Chem. Phys.* **1997**, *107*, 8064−8072.
(70) Nozik, A. J.; Memming, R. *J. Phys. Chem.* **1996**, *100*, 13061−13078.
(71) Kamat, P. V.; Bedja, I.; Hotchandani, S.; Patterson, L. K. *J. Phys. Chem.* **1996**, *100*, 4900−4908.
(72) Liu, D.; Kamat, P. V.; George Thomas, K.; Thomas, K. J.; Das, S.; George, M. V. *J. Chem. Phys.* **1997**, *106*, 6404−6410.
(73) Nasr, C.; Hotchandani, S.; Kamat, P. V. *J. Phys. Chem. B* **1998**, *102*, 4944−4951.